



FLOW VISUALIZATION OF MULTIPHASE FLOW SYSTEMS

Muthanna Al-Dahhan¹

1: Associate Professor, Associate Director of the Chemical Reaction Engineering Laboratory
Chemical Engineering Department, Washington University
St. Louis, MO 63130, USA

muthanna@che.wustl.edu

ABSTRACT

Multiphase flow systems such as multiphase reactors are widely used in various industrial processes. These reactors are opaque. To advance their design, scale-up and performance prediction non-invasive measurement techniques are needed to properly understand their hydrodynamics and to visualize their flow field. In our laboratory, gamma ray computed tomography (CT) and computer automated radioactive particle tracking (CARPT) have been used to study various types of multiphase flow systems such as bubble column, slurry bubble columns, liquid-solid riser, stirred tank, packed bed, photobioreactor, etc. and to obtain data in a non-invasive manner for validation of computational fluid dynamic (CFD) models. These techniques and selected results at glance will be presented.

Keywords: *multiphase reactors, flow visualization, non-invasive measurement techniques*

المفاعلات المتعددة الحالات تستخدم بشكل واسع في مختلف العمليات الصناعية. تصاميم و حساب اداء هذه المفاعلات يتطلب استخدام اجهزة متقدمه لدراسه طبيعتها الهيدروديناميكيه و تركيبه جريان الموائع فيها بحيث لا تؤثر على جريان و طبيعه المواد داخلها. في مختبرنا اُنشانا و استخدمنا جهاز المسح الشعاعي و جهاز متابعه جزيئه مشعه لدراسه عده انواع من المفاعلات التي تحوي على حالتين أو ثلاث حالات من الغاز ، السائل، و الصلب. هذه الأجهزه المتقدمه و إستخداماتها مع بعض الأنتائج سوف تشرح هنا بشكل ملخص.

1. INTRODUCTION

Multiphase flow systems are used extensively in industry. Examples of these systems are multiphase reactors which find applications in many processes such as petroleum refining, synthesis gas conversion to fuels and chemicals, bulk commodity chemicals, specialty chemicals (pharmaceutical, herbicides, pesticides), conversion of undesired byproducts into recyclable products, manufacture of polymers, biochemical, and environmental. In the US alone, the value of shipments generated by industry that employs multiphase flow systems is estimated to be more than 640 billion dollars a year (Mills, 2001). Different configurations

for phases interaction exist in multiphase reactors, for example bubble column (gas-liquid interaction), slurry bubble column (gas-liquid-fine solids catalyst interaction), liquid-solid riser and fluidization (liquid-solids interaction), gas-solid riser and fluidization (gas-solids interaction), ebullated beds (gas-liquid-solids catalyst interaction), and packed beds (gas-liquid-solids catalyst interaction). In general, multiphase reactors represent the heart of any process. Since the reactor performance determines the number, size, and type of the needed units in front or after the reactor and hence dictates the economics of plant process. Therefore, it is essential to quantify different reactor performance parameters such as conversion, selectivity, production, yield, etc. as a function of the design and operating parameters which require proper descriptions of the transport-kinetic interactions on various scales.

However, the design, scale-up and performance prediction of these multiphase flow systems are still challenging tasks due to the enormous complexity of their flow field interacting phenomena. Hence, reactor scale phenomena of phases distribution, phases recirculation, backmixing and hydrodynamic and transport parameters are critical in sizing the reactor properly for achieving optimal performance. Accordingly, a more fundamental understanding of the fluid dynamics and transport of these reactors is needed in order to advance their scale-up, design and performance. This is a challenging task since these systems are opaque and one cannot "see" into them. Therefore, the commonly used sophisticated optical techniques such as laser-doppler velocimetry (LDV), digital particle image velocimetry (PIV), etc. cannot be pursued for hydrodynamics and mixing investigations of such opaque systems. In general, the desirable characteristics in any experimental diagnostic and measurement techniques are: 1) good spatial resolution in both velocity and volume fraction (holdup) measurements, 2) capability to provide instantaneous (snapshot) measurements so that one could, in principle, be able to quantify the turbulent and dynamic flow structure, 3) ability to probe opaque systems in which the dispersed phase volume fractions are high, 4) statistically reproducible results obtainable in a finite time, 5) amenability to automation, so as to minimize human involvement in the data collection process, 6) portability of the technique to larger units, such as pilot plant and industrial locations, and 7) safety of the personnel involved in the experimentation. At present, no single experimental technique satisfies all these characteristics. However, research in the direction of the long term goal to achieve the above requirements is constantly in progress (Chaouki, et al., 1997). As a result, many non-invasive diagnostic and measurement techniques have been developed such as particle image velocimetry (PIV), laser doppler anemometry (LDA), magnetic resonance imaging (MRI), gamma ray camera (GRC), positron emission tracking and tomography (PET), γ -ray particle tracking, densitometry, electrical capacitance, resistance and impedance tomography (ECT, ERT, EIT), ultrasound tomography, X-ray tomography, gamma ray (γ -ray) tomography, etc. Among these techniques, two non-invasive advanced diagnostic techniques, namely, γ -ray computed tomography (CT) and computer automated radioactive particle tracking (CARPT), have been used in our laboratory to advance the fundamental understanding of the flow

pattern, mixing, and turbulent parameters of the various types of multiphase flow systems. In addition, in our laboratory, the unique findings have been used to advance the scale-up methodology, modeling, and computation fluid dynamic (CFD) simulations of the reactors/systems studied (For example, see [Degaleesan, 1997], [Rados, 2002], [Chen, et al., 1998, 1999], [Kemoun et al., 2000], [Wu et al., 2001], and many others).

In this presentation, CT and CARPT techniques will be discussed. Recent results at a glance obtained in our laboratory by these techniques for various multiphase flow systems including bubble column, slurry bubble column, stirred tank reactor, ebullated bed, bioreactor, etc. will be presented. Our findings obtained by CT and CARPT have been used to advance the design, scale-up, modeling and CFD validation of these reactors. A brief description of CT and CARPT and their results at glance obtained in an air-lift photobioreactor for the growth of high value produces microalgae are outlined below.

1.1. Computed Tomography (Ct)

CT is used to measure the time average phase holdup distribution at any desired cross-section of a two-phase flow system (e.g. gas-liquid, liquid-solid, gas-solid). A collimated hard source (100 mCi of Cs-137) is positioned opposite to 2" sodium iodide detectors in a fan beam arrangement as shown in Figure 1 [Kumar, 1994]. The number of detectors depends on the diameter of the reactor (e.g. 5 detectors for 6 inch diameter column). The lead collimators in front of the detectors have manufactured slits and the lead assembly can move so as to allow repeated use of the same detectors for additional projections. A 360 ° scan can be executed at any desired location. In the current configuration, columns from 2" to 18" in diameter can be scanned. Because of the different attenuation due to each phase, the distribution phases in a scanned cross-section can be calculated from the measured attenuation of the beams of radiation projections through the two phase mixture. With the current CT unit, we have achieved a spatial resolution of approximately 1-2 mm and density resolution of about $<0.04 \text{ gm/cm}^3$. A slight error in the measurement is encountered in the region close to the wall particularly if the wall consist of high attenuation materials (e.g. stainless steel). A complete cross-section requires a long time to scan (about 2 hours), and hence only measurements of time-averaged density distributions are achievable. Estimation-maximization algorithms (E-M) are used, which we found to be superior compared to convolution, filtered back projection and algebraic reconstruction [Kumar, 1994].

1.2. Computer Automated Radioactive Particle Tracking (Carpt)

In CARPT, a single radioactive particle that is dynamically similar to the phase to be traced is introduced into the system. When solid motion is monitored in ebullated beds, fluidized beds or slurries, a composite particle of the same size and density as the solids in the system is

prepared. For monitoring of liquid motion a neutrally buoyant particle is made. CARPT calibration is performed in situ at the same operating conditions of the CARPT experiment by positioning a tracer particle, which is usually Sc-46 of 200 – 500 μCi strength, at over 1000 known locations and recording the counts obtained at each detector to generate counts-position maps. Once the calibration is completed, the tracer particle is let loose in the system and the operating conditions are controlled and kept constant for many hours while the particle is tracked. Sampling frequency is adjusted to assure good accuracy. Typically, it is selected at 50 Hz for bubble columns since the finite size particle used as tracer cannot capture motion of frequencies above 25 Hz [Degaleesan, 1997]. A wavelet based filtering algorithm [Degaleesan, 1997] is employed to remove the noise in position readings created by the statistical nature of gamma radiation. The processing of data proceeds along the lines shown in Figure 2. From filtered particle positions at subsequent times the instantaneous velocity is calculated and assigned to the volume element (a compartmental grid is pre-established for the column) into which the midpoint falls. As shown in Figure 3, the projection of the particle trajectories in the vertical plane shows how much more rapidly the particle moves in the flow (extent of mixing and stagnant zones) with respect to superficial gas velocity and flow regime. The resolution of CARPT is ~ 3 mm in the wall region. Due to the wall attenuation, slightly larger error is encountered in the particle positions reconstruction of the calibration points in the wall region. The data collection continues until adequate statistics are obtained. For each compartment (cell) ensemble average velocities are evaluated and from the difference between instantaneous and average velocities fluctuating velocities vectors are calculated. This allows evaluation of most important Eulerian auto-correlations and cross-correlations. Kinetic energy and components of the Reynolds “like” stresses are obtained. Most importantly Lagrangian auto-correlation lead to the evaluation of the eddy diffusivities via first-principles [Degaleesan, 1997; Chen, et al., 1999]. In addition to the “Eulerian” interpretation of the data, the particle position and velocity time series that form the raw data from a CARPT experiment is rich in Lagrangian information about mixing on local spatial and temporal scales. The estimated errors in the measured quantities vary with the operating conditions used. For example, for superficial gas velocity of about 45 cm/s in air-water-glass beads (150 μm) system the estimated error in the averaged axial velocity is less than 3 cm/s and in the averaged radial velocity is less than 0.2 cm/s. However, the error in Reynolds “like” shear stresses is about less than $10 \text{ cm}^3/\text{s}^2$.

1.3. Results At A Glance

Figure 4 shows a sample of the recent results at a glance obtained in an air-lift photobioreactor for microalgae growth to study its hydrodynamics and their impact on the cell movement and the reactor performance.

REFERENCES

1. Chaouki, J., Larachi, F., Dudukovic, M.P. (Eds.), 1997, "Non-Invasive Monitoring of Multiphase Flows," Elsevier, Amsterdam.
2. Chen, J., 1999, "Comparative Hydrodynamics Study in a Bubble Column Using Computer Automated Radioactive Particle Tracking (CARPT)/Computed Tomography (CT) and Particle Image Velocity (PIV)," *Chemical Engineering Science*, 54, pp 2199-2207.
3. Chen, J., 1999, "Fluid Dynamic Parameters in Bubble Columns with Internals," *Chemical Engineering Science*, 54, pp 2187-2197.
4. Chen, J., 1998, "Gas Holdup in Large Diameter Bubble Columns Measured by Computed Tomography," *Flow Measurement and Instrumentation*, 9, pp 91-101.
5. Degaleesan, S., 1997, "Fluid Dynamic Measurements and Modeling of Liquid Mixing in Bubble Columns," D.Sc. Thesis, Washington University, St. Louis, Missouri, USA.
6. Gupta, P., 2001, "Comparison of Single- and Two-Bubble Class Gas-Liquid Recirculation Models – Application to Pilot-Plant Radioactive Tracer Studies During Methanol Synthesis," *Chemical Engineering Science*, 56, pp 1117-1125.
7. Kemoun, A., 2000 "Gas Holdup in Bubble Columns at Elevated Pressure via Computed Tomography," *International Journal of Multiphase Flow*.
8. Kumar, S.B., 1994, "Computed Tomographic Measurements of Void Fraction and Modeling of the Flow in Bubble Columns," Ph.D. Thesis, Florida Atlantic University, Boca Raton, FL, USA.
9. Rados, N., 2002, "Slurry Bubble Column Hydrodynamics", D.Sc. Thesis, Washington University, St. Louis, Missouri, USA.
10. Wu, Y. and M.H. Al-Dahhan, 2001, "Prediction of Axial Liquid Velocity Profile in Bubble Columns," *Chemical Engineering Science*, 56(3), pp 1127-1130.
11. Mills, P.L., 2001, "Recent Development and Advances in Laboratory-Scale Multiphase Reactors," Plenary Lecture, First North American Symposium on Chemical Reaction Engineering (NASCRE1), Houston, TX.
12. Wu, Y., Ong, B., Al-Dahhan, M.H., 2001, "Predictions of Radial Gas Holdup Profiles in Bubble Column Reactors," *Chemical Engineering Science*, 3, pp 1207-1210.

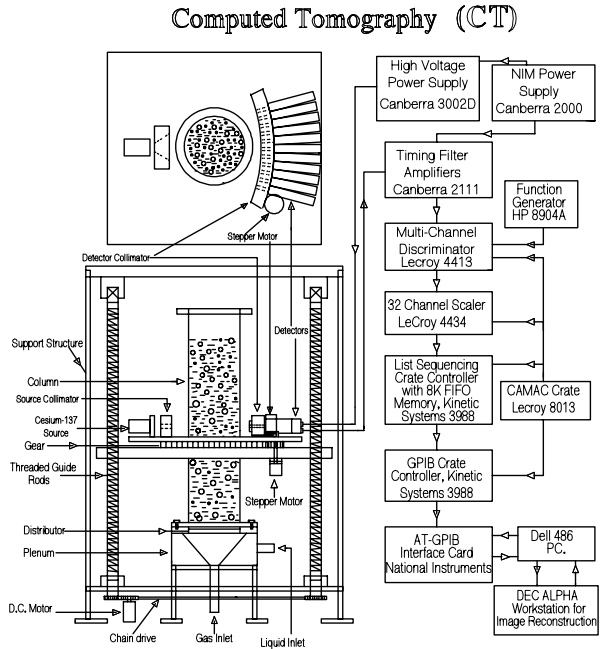


Figure 1: Schematic Diagram of CREL Computed Tomography (CT)

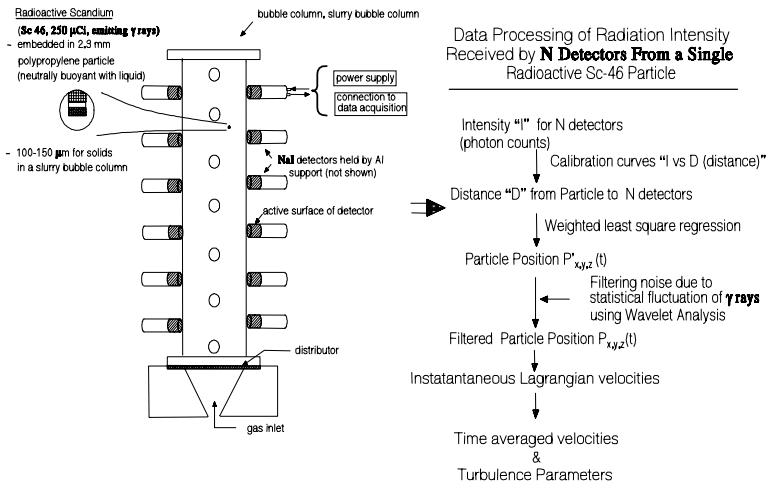


Figure 2: Schematic Diagram of CREL Computer Automated Radioactive Particle Tracking (CARPT)

For the entire 3 dimensional flow field:

- Lagrangian velocities
- Ensemble/time averaged velocities
- Turbulent Reynolds stresses
 - Normal: $\overline{u_r u_r}, \overline{u_\theta u_\theta}, \overline{u_z u_z}$
 - Shear: $\overline{u_r u_\theta}, \overline{u_r u_z}, \overline{u_\theta u_z}$
- Turbulent kinetic energy $k = \frac{1}{2} (\overline{u_r^2} + \overline{u_\theta^2} + \overline{u_z^2})$
- Turbulent eddy diffusivities
 - Radial: $D_r(t) = \frac{1}{2} \frac{d}{dt} \overline{y_r^2(t)} = \int_0^t \overline{v_r(t) v_r(\tau)} dt = \int_0^t R_{rr}(\tau) dt$
 - Axial: $D_z(t) = \frac{1}{2} \frac{d}{dt} \overline{y_z^2(t)} = \int_0^t \left\{ \overline{\frac{\partial u_z}{\partial x}} \Big|_{y_r(t)} \left[\int_0^r v_z(t) v_z(\tau) dt \right] + \overline{v_z(t) v_z(t')} \right\} dt$
 $= \int_0^t \overline{\frac{\partial u_z}{\partial x}} \Big|_{y_r(t)} \left[\int_0^r R_{zz}(\tau) dt' \right] dt + \int_0^t R_{zz}(t') dt'$

Particle Lagrangian Trajectory from CARPT in a 6" Column

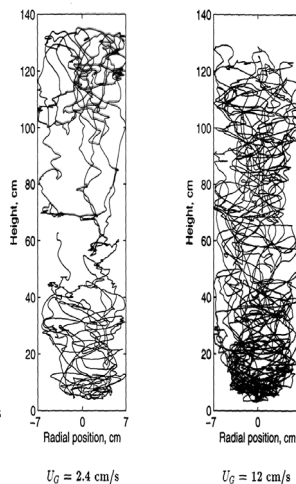


Figure 3: Liquid Fluid Dynamic Quantities Directly Obtainable from CARPT Measurements

